PROCEEDINGS OF SCIENCE

Strong coupling constant and heavy quark masses in (2+1)-flavor QCD

Johannes Heinrich Weber*
Michigan State University
Department of Computational Mathematics, Science and Engineering & Department of Physics and Astronomy
E-mail: weberjo8@msu.edu

We present lattice determinations of the heavy quark masses and the strong coupling constant obtained by two different methods in (2+1)-flavor QCD with Highly Improved Staggered Quark (HISQ) action. Using lattice calculations of the moments of the pseudoscalar quarkonium correlators at several values of the heavy valence quark mass we determine the strong coupling constant in $\overline{MS}$ scheme at four low energy scales corresponding to m_c, $1.5m_c$, $2m_c$ and $3m_c$, with m_c being the charm quark mass. We obtain $\Lambda_{\overline{MS}}^{n_f=3} = 298 \pm 16$ MeV, which is equivalent to $\alpha_s(\mu = M_Z, n_f = 5) = 0.1159(12)$. For the charm and bottom quark masses in $\overline{MS}$ scheme we obtain: $m_c(\mu = m_c, n_f = 4) = 1.265(10)\,\mathrm{GeV}$ and $m_b(\mu = m_b, n_f = 5) = 4.188(37)\,\mathrm{GeV}$. Using lattice calculations of the QCD static energy at $T = 0$, or the static singlet free energy at $T > 0$ we obtain $\alpha_s(M_Z) = 0.11660^{+0.00110}_{-0.00056}$, or $\alpha_s(M_Z) = 0.11638^{+0.00095}_{-0.00087}$. The novel feature of our analyses that many lattice spacings are used in the continuum extrapolations, with the smallest lattice spacings at $T = 0$, or at $T > 0$ being $a = 0.025\,\mathrm{fm}$, or $a = 0.008\,\mathrm{fm}$, respectively.

37th International Symposium on Lattice Field Theory - Lattice2019
16-22 June 2019
Wuhan, China

*Speaker.

PoS(LATTICE2019)101

1. Introduction

The strong coupling constant and quark masses are important parameters of the Standard Model (SM), and thus their knowledge is required for its testing. Lattice QCD calculations play an increasingly important role in the determination of the quark masses and α_s because of the increase in the available computational resources and algorithmic improvements in recent years.

For the lattice determination of α_s one calculates a quantity $O(\nu)$ that depends on a physical scale ν nonperturbatively on the lattice and compares it with the corresponding perturbative power series in $\alpha_s(\nu)$. One thus obtains the value of $\alpha_s(\nu)$ if the truncated power series in $\alpha_s(\nu)$ is sufficiently accurate for $O(\nu)$. This leads to the so-called window problem: ν has to be smaller than the lattice cutoff, a^{-1}, to avoid large discretization artifacts, yet large enough to make the perturbative expansion accurate, i.e. $\Lambda_{\mathrm{QCD}} \ll \nu \ll a^{-1}$.

Hence, very fine lattices are required, and controlling the discretization artifacts is the key obstacle in this endeavor. We focus on this challenge in the following discussion of the QCD static energy and the moments of quarkonium correlators in (2+1)-flavor QCD with the HISQ action. The $T = 0$ gauge ensembles underlying both calculations have been generated for the study of the (2+1)-flavor QCD equation of state [1, 2], and suffer from rather small spatial volumes and rather short Euclidean time directions. Moreover, since the bulk properties in the QCD thermodynamics have only a relatively mild dependence on the sea quark masses, the light sea quark masses are not fixed at the physical point, but at $m_l = m_s/20$ or $m_l = m_s/5$. In Sec. 2 we discuss the determination of α_s from the QCD static energy. In Sec. 3 we discuss the determination of α_s and heavy quark masses from the moments of quarkonium correlators. Finally, Sec. 4 contains our conclusions.

2. Static energy and static singlet free energy

The QCD static energy $E(r)$ of a $q\bar{q}$ pair, which depends on α_s already at the tree level, is an observable up to an additive constant. The static $q\bar{q}$ are strictly immobile, and their displacement $\boldsymbol{r}$ is a well-defined quantum number. $E(r)$ is a function of r, of the QCD coupling $\alpha_s = g^2/4\pi$, and of the masses of the N_f sea quarks. $E(r)$ is defined in terms of the large time limit of the expectation value of the time derivative of the Wilson loop $W_S(r,t)$. $W_S(r,t)$ has a self-energy divergence proportional to its circumference. While $W_S(r,t)$ can be defined as a smooth path-ordered contour in the continuum, $W_S(\boldsymbol{r},t) = \exp\left[ig \oint_{\boldsymbol{r},t} dz^\mu A_\mu\right]$, it has to be defined as a rectangular Wilson loop on the lattice. Thus, there are additional cusp divergences, and the spatial lines introduce a path dependence on the lattice. Both issues may be ameliorated through link smearing. $E(r)$ cannot depend on the fields at infinite time separation. Hence, $E(r)$ may be defined as well through the spatial correlator of two temporal Wilson lines in Coulomb gauge. The definition in terms of this correlator avoids the cusp divergences, or the self-energy divergences and path dependence associated with the spatial distance between the two Wilson lines. A similarly constructed thermal correlator at the time equal to the inverse temperature $\tau = aN_\tau = 1/T$ defines the static singlet free energy $F_S(r/a,T)$. $F_S(r,T)$ is very similar to $E(r)$ for $r \ll 1/T$. The details depend on the scale hierarchy, i.e. $1/r \gg \alpha_s/r \gg T \gg m_D \sim gT$ or $1/r \gg T \gg m_D \sim gT \gg \alpha_s/r$. The result at order g^5 for the second hierarchy [3] is within uncertainties compatible with the lattice throughout the accessible temperature range [4]. Thermal effects are known to be strongly suppressed for the first hierarchy, although no perturbative result is available. For a detailed discussion of the hierarchies see Ref. [5].

Since the lattice has a reduced symmetry (cubic group W_3 instead of rotation group $O(3)$), there is only a finite set of displacements between the static $q\bar{q}$ that are geometrically equivalent. $E_{\text{lat}}(\boldsymbol{r})$ is accessible on the lattice for $r = \sqrt{n_x^2+n_y^2+n_z^2}a$, and $n_x,\ n_y,\ n_z = 0,\ 1,\ 2,\ \ldots$. In order to resolve small r, fine lattice spacings a are indispensable. For $r \sim a$ the lattice result $E_{\text{lat}}(\boldsymbol{r})$ is affected by severe discretization artifacts. The origin of these artifacts is apparent from the fact that the paths connecting the static $q\bar{q}$ belong to different representations of W_3. For $r/a \gtrsim 5$ the artifacts of $E_{\text{lat}}(\boldsymbol{r})$ are usually of a similar size as the statistical errors, and thus cannot be resolved clearly. These artifacts can be understood to a large extent in terms of the tree-level calculation,

$$E^{\text{tree}}_{\text{lat}}(\boldsymbol{r}) = -C_F g^2 \int \frac{d^3k}{(2\pi)^3}\, D_{00}(\boldsymbol{k},k_0=0)\, e^{\mathrm{i}\boldsymbol{k}\cdot\boldsymbol{r}}, \tag{2.1}$$

i.e. one-gluon exchange for a static $q\bar{q}$ pair without running coupling. These artifacts are due the gluon propagator $D^{-1}_{00}(\boldsymbol{k},k_0=0) = \sum_{j=1}^{3} \sin^2\left(\frac{ak_j}{2}\right) + c_w \sin^4\left(\frac{ak_j}{2}\right)$, where $c_w = 0$ or $c_w = 1/3$ are for the Wilson and Lüscher-Weisz (LW) actions, respectively. In the continuum Eq. (2.1) yields $E^{\text{tree}}_{\text{cont}}(r) = V^{\text{tree}}_s(r) = -C_F\alpha_s/r$. A tree-level improved distance r_{I} is defined by equating $E^{\text{tree}}_{\text{lat}}(\boldsymbol{r}) \equiv -C_F\alpha_s/r_{\text{I}} = E^{\text{tree}}_{\text{cont}}(r_{\text{I}})$, where r_{I} depends on the path geometry, i.e. paths belonging to different representations of W_3 correspond to unequal tree-level improved distances r_{I}. This assignment is called the tree-level correction (TLC). These improved distances r_{I} differ from the naive (bare) distances by up to 8% or 4% (at $r/a = 1$) for the Wilson or LW actions. On the one hand, TLC reduces the size of the residual artifacts of $E^{\text{QCD}}_{\text{TLC}}(\boldsymbol{r})$ to the level of the typical statistical errors in lattice simulations already at distances $r/a \gtrsim 3$. On the other hand, TLC accounts for the largest part of the artifacts of $E^{\text{QCD}}_{\text{TLC}}(\boldsymbol{r})$ even at distances $r/a \lesssim 3$, since the coupling $\alpha_s(1/r)$ is small at short distances. A similar pattern of artifacts still remains for $E^{\text{QCD}}_{\text{TLC}}(\boldsymbol{r})$. One may use an estimate for $E^{\text{QCD}}_{\text{cont}}(r)$, and calculate the necessary nonperturbative correction (NPC) beyond TLC. This has been achieved in two schemes that yield consistent answers. First, each distance r corresponds to different r/a on fine or coarse grids. Thus, $E^{\text{QCD}}_{\text{TLC}}(\boldsymbol{r})$ on fine lattices (at large enough distances) may serve as a continuum estimate for determining the residual artifacts of $E^{\text{QCD}}_{\text{TLC}}(\boldsymbol{r})$ on coarser lattices. This scheme has a systematic uncertainty as it requires interpolating $E^{\text{QCD}}_{\text{TLC}}(\boldsymbol{r})$ on fine grids to distances r where $E^{\text{QCD}}_{\text{TLC}}(\boldsymbol{r})$ is available on coarse grids. The other drawback is that this scheme lacks information for small r/a on fine lattices (most important for comparison to weak coupling). Second, one may compare to the weak-coupling result $E(r)$ directly to estimate the correction. In this scheme, the weights of the data where corrections are needed must be reduced by hand, and one has to marginalize over the details of the utilized weak-coupling result. Lastly, the comparison must be restricted to the perturbative window, i.e. following [6] to $r \lesssim 0.5\,r_1$. Due to the a^2 errors of the gauge action, the artifacts of $E^{\text{QCD}}_{\text{TLC}}$ must be $\alpha^n_s\ (a/r)^{2m}$, where $m,n \geq 1$. Namely, the artifacts for fixed r/a are polynomials in the bare coupling α^{bare}_s. The nonperturbative corrections from either of these estimates may be extrapolated in the gauge coupling $\alpha^{\text{lat}}_s = \alpha^{\text{bare}}_s/u_0^4$ (tadpole-improved using the plaquette, $u_0 = \left\langle U_{\mu\nu}\right\rangle^{1/4}$) towards the continuum. Corrections of the order $(\alpha^{\text{lat}}_s)^2$ are required for $r/a < 2$, while the order α^{lat}_s is sufficient for $2 \leq r/a < \sqrt{8}$ at the present numerical accuracy. $E^{\text{QCD}}_{\text{NPC}}(\boldsymbol{r}) \simeq E^{\text{QCD}}_{\text{NPC}}(r)$ for all β is statistically consistent up to the divergent, additive constants.

The calculation of α_s from $E^{\text{HISQ}}_{\text{lat}}(r)$ at $T = 0$ is straightforward. $E(r)$ in any two regularization scheme differs by a constant, which is different for each β and has to be determined through a fit. First, $E^{\text{HISQ}}_{\text{lat}}(r)$ must be at small enough r that the perturbative expansion shows apparent convergence, which is satisfied for $r \lesssim 0.5\,r_1$ [6]. In this range the sea quark mass effects can be neglected.

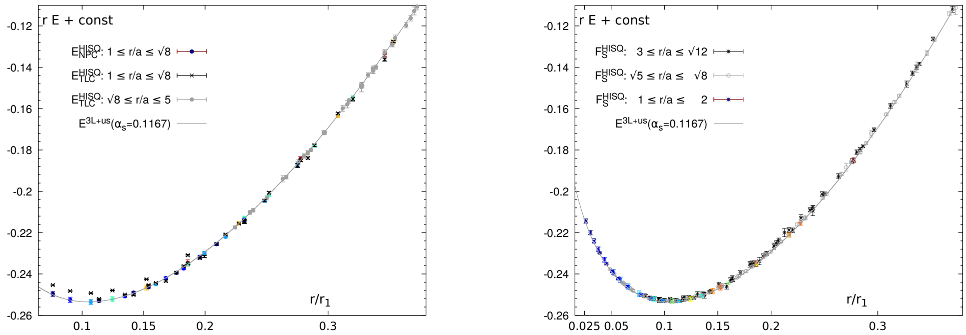

Figure 1: The nonperturbative lattice and the perturbative continuum results for $E^{\mathrm{QCD}}(r)$ multiplied by the distance, $rE(r)$. (left) The $T = 0$ data [5] are NPC (colored bullets) or TLC (black crosses and gray bullets). The colors indicate different lattice spacings of the NPC data. The line represents the three-loop result with resummed leading ultrasoft logarithms, Eq. (3) in Ref. [5], corresponding to the central value $\alpha_s(M_Z) = 0.1167$ of the analysis of the $T = 0$ data with $r/a \geq \sqrt{8}$ (gray bullets). The $T = 0$ NPC data with $r/a < \sqrt{8}$ are well-aligned with the fit excluding these data, while the $T = 0$ TLC data with $r/a < \sqrt{8}$ cannot be consistently described by a continuum result for any value of $\alpha_s(M_Z)$. (right) The $T > 0$ NPC data [5] in different r/a windows are fully compatible with the same continuum result.

Second, one has to ensure that the artifacts can be neglected, i.e. use $E^{\mathrm{HISQ}}_{\mathrm{TLC}}(r)$ or $E^{\mathrm{HISQ}}_{\mathrm{NPC}}(r)$. Then one may simply compare the lattice result with N_f sea quarks to the weak-coupling result with N_f massless quarks with a fit of $1+N_\beta$ parameters, with N_β being the number of ensembles used. $E^{\mathrm{HISQ}}_{\mathrm{NPC}}(r)$ with up to six lattice spacings $0.08\,r_1 \leq a \leq 0.20\,r_1$ [5] yields for $0.076\,r_1 \leq r \leq 0.24\,r_1$

$$\alpha_s(M_Z) = 0.11660^{+0.00110}_{-0.00056}, \qquad \delta\alpha_s(M_Z) = (41)^{\mathrm{stat}}(21)^{\mathrm{lat}}(10)^{r_1}(^{+95}_{-13})^{\mathrm{soft}}(28)^{\mathrm{us}}. \tag{2.2}$$

Our result confirms that the nonperturbative correction captures the residual artifacts well, see Fig. 1 (left). After meeting the same two conditions as at $T = 0$, and restricting to $r \ll 0.3/T$, one may simply compare the $T > 0$ lattice data with the weak-coupling result at $T = 0$ in a similar fit of $1+N_\beta$ parameters. The result is consistent with the $T = 0$ calculation. $F^{\mathrm{HISQ}}_S(r,T)$ with up to fifteen lattice spacings $0.027\,r_1 \leq a \leq 0.20\,r_1$ [5] yields for $0.026\,r_1 \leq r \leq 0.1\,r_1$

$$\alpha_s(M_Z) = 0.11638^{+0.00095}_{-0.00087}, \quad \delta\alpha_s(M_Z) = (80)^{\mathrm{stat}}(21)^{\mathrm{lat}}(17)^{T>0}(10)^{r_1}(^{+40}_{-06})^{\mathrm{soft}}(15)^{\mathrm{us}}. \tag{2.3}$$

In order to escape a possible contamination by $T > 0$ effects the analysis was performed with $r/a \leq 2$, which rendered use of the nonperturbative correction inevitable. Analysis with $r/a \leq \sqrt{8}$ or $r/a \leq \sqrt{12}$ would produce a similar result with smaller errors, see Fig. 1 (right). The uncertainty due to the $T > 0$ calculation has been estimated by comparing the results obtained with $N_\tau = 12$, or $N_\tau = 16$ with each other, or with the $T = 0$ for the same upper limit of the distance window both in terms of r/a and r/r_1. The error budget is discussed in detail in Ref. [5]. All estimates of the perturbative uncertainty are dramatically reduced when the comparison is restricted to the smaller maximal distance r, while the central value hardly depends on the fit range for $r \lesssim 0.45\,r_1$.

3. Moments of quarkonium correlators

Due to the periodic boundary condition in time that is used in most QCD lattice calculations, which implies a backward propagating contribution, the time moments on the lattice are defined as

$$G_n(a,V) = \sum_{t=0}^{N_\tau/2} t^n \left\{ G(t,a,V) + G(N_\tau - t,a,V) \right\}, \tag{3.1}$$

PoS(LATTICE2019)101

where $G(t,a,V)$ is the local, renormalization group invariant (rescaled with the square of the bare heavy quark mass am_{h0}) pseudoscalar quarkonium correlator on the lattice with volume V, where $t=\tau/a$ is the Euclidean time in units of the lattice spacing, a. $G_n(a,V)$ is finite for $n\geq 4$, since $G(t,a,V)$ diverges as t^{-4}. Larger values of m_h result in larger discretization artifacts $(am_h)^n$ for $G_n(a,V)$. It is clear from Eq. (3.1) that, on the one hand, smaller n implies more sensitivity to the artifacts of the correlator at small times $\tau\sim a$, whereas, on the other hand, larger n implies more sensitivity to finite N_τ effects. It is favorable to consider the reduced moments R_n in the lattice calculation [7], where the R_n are ratios of the moments in QCD and in the free theory,

$$R_n(a,V,m_h)=\left[\frac{G_n^{\mathrm{QCD}}(a,V,m_h)}{G_n^{(0)}(a,V,m_h)}\right]^{p_n}, \quad p_n=\begin{cases}1 & (n=4)\\ \frac{1}{n-4} & (n>4)\end{cases}. \tag{3.2}$$

There are various cancellations between systematic effects in these ratios. These cancellations are particularly relevant wrt the effects of the lattice spacing a, of the heavy quark mass m_h, and of the periodic time direction, and to some extent, wrt the finite volume V, too. In particular, the tree-level contribution to the artifacts, $\alpha_s^0 a^n$, cancels exactly in the reduced moments for all n. Moreover, the uncertainties of G_n in QCD and in the free theory due to the error of the numerical tuning of am_{h0} are subject to a strong compensation in R_n. The contribution for $t>N_\tau/2$ is missing both in the numerator and denominator. It is possible to account for this by replacing the correlator for large t with $\cosh[am_0(t-N_\tau/2)]$, where m_0 is the ground state mass and N_τ is sufficiently large. In the free theory it is easy to calculate directly at large enough N_τ such that finite N_τ effects can be neglected. A general parametrization of the finite volume error is

$$\frac{R_n(\infty)-R_n(V)}{R_n(V)}=\left(\left[\frac{\delta_V G_n^{\mathrm{QCD}}(V)}{G_n^{\mathrm{QCD}}(V)}\right]-\left[\frac{\delta_V G_n^{(0)}(V)}{G_n^{(0)}(V)}\right]\right)\times\begin{cases}1 & (n=4)\\ \frac{1}{n-4} & (n>4)\end{cases}, \tag{3.3}$$

but simplifies under the reasonable assumption that the free field theory result is much more sensitive to the finite volume effects, i.e. that the first term in square brackets can be neglected. Estimating $\delta_V G_n^{(0)}(a,V,m_h)$ via free field theory calculations using multiple box sizes is straightforward. Lastly, it is attractive to consider the ratios of the reduced moments, since statistical fluctuations and the errors due to the numerical tuning of the heavy quark mass cancel in these ratios to a large extent. A similar compensation may happen to a lesser extent as well for the discretization artifacts, for the effects of the periodic time direction, and for the finite volume effects.

The moments of quarkonium correlators are known in the $\overline{\mathrm{MS}}$ scheme at order α_s^3. Quarkonium correlators also receive nonperturbative contributions, the one due to the gluon condensate [8] being the largest. Thus, the reduced moments $R_n[\alpha_s(\nu),m_h(\nu_m),\langle\frac{\alpha_s}{\pi}G^2\rangle]$ can be written as

$$R_n=\left(1+\sum_{j=1}^{3}r_{nj}\left[m_h(\nu_m),\frac{\nu}{m_h(\nu_m)}\right]\left[\frac{\alpha_s(\nu)}{\pi}\right]^j+\frac{11}{4}\frac{\langle\frac{\alpha_s}{\pi}G^2\rangle}{m_h^4(\nu_m)}\right)\times\begin{cases}1 & (n=4)\\ \left(\frac{m_{h0}}{m_h(\nu_m)}\right) & (n>4)\end{cases}, \tag{3.4}$$

where the gluon condensate is known from τ decays [9], $\langle\frac{\alpha_s}{\pi}G^2\rangle=-0.006(12)\,\mathrm{GeV}^4$. $m_h(\nu_m)$ is the $\overline{\mathrm{MS}}$ heavy quark mass at the scale ν_m, and $\alpha_s(\nu)$ is the $\overline{\mathrm{MS}}$ strong coupling constant at the scale ν. In principle the renormalization scales ν and ν_m could be different [10], although most studies assume $\nu=\nu_m$. For this choice $\nu=\nu_m=m_h$ the coefficients $r_{nj}(m_h(\nu_m),\nu/m_h(\nu_m))$ simplify to mass-independent constants r_{nj} of order one without any evident pattern, see Tab. 2 of Ref. [12]. There are indications that the independent variation of ν and ν_m leads to significantly increased uncertainty estimates [11]. Finite size effects tend to be the dominant systematic uncertainties for

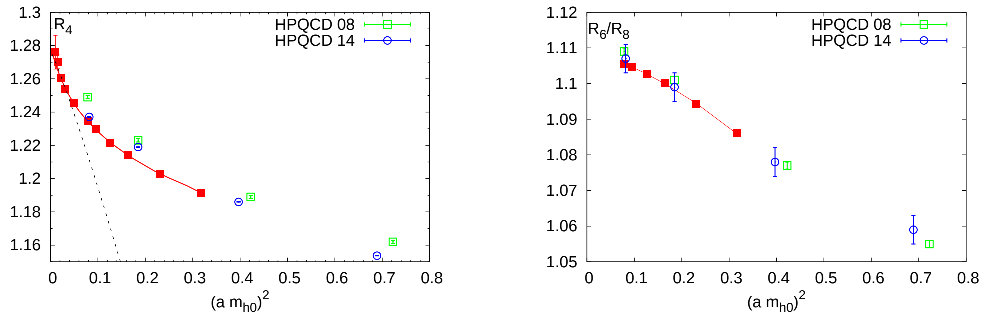

Figure 2: The lattice spacing dependence of the reduced moment R_4, or of the ratio R_6/R_8 with the HISQ action at the valence charm quark mass. The red filled squares correspond to the most recent (2+1)-flavor HISQ result, PW19 [12], and clearly resolve the logarithmic lattice spacing dependence. The green open squares correspond to the HISQ on (2+1)-flavor asqtad result, HPQCD08 [7], while the blue open circles correspond to the (2+1+1)-flavor HISQ result, HPQCD14 [13]. The most simple fit of R_4 using only $\alpha_s^{\rm lat}\ (am_h)^2$ (black dashed line) is only feasible for $a \lesssim 0.04\,$fm.

the finer lattices, whereas the mis-tuning of the heavy quark masses tends to be the dominant systematic uncertainty for the coarser lattices. The valence heavy quark masses were tuned with the spin-average of the pseudoscalar and vector channels for the $m_l = m_s/20$ ensembles, and with just the pseudoscalar mass for the very fine $m_l = m_s/5$ ensembles. Quarkonium correlators on ensembles with different strange sea quark masses indicate that sea quark mass effects are comparable to the statistical or systematic errors, i.e. they are statistically insignificant, and thus can be neglected.

With the exception of the contributions from the condensates, which are from the scale $\Lambda_{\rm QCD}$, or from the even lower and less important scales of the sea quark masses, the relevant scale in the problem is the heavy quark mass m_{h0}. As the contribution from the condensates has 200% uncertainty in the continuum, and is suppressed by four powers of the heavy quark mass, cf. Eq. (3.4), the associated discretization errors are negligible and cannot be resolved in the analysis. Hence, in the infinite volume limit the most general fit form for the discretization artifacts is given by

$$R_n(a,m_h) - R_n(0,m_h) = \sum_{n=1}^{N} \sum_{j=1}^{J} c_{nj}\ (\alpha_s^{\rm lat})^j\ (am_{h0})^{2n}, \tag{3.5}$$

where the c_{nj} are constants. The gauge coupling $\alpha_s^{\rm lat} = \alpha_s^{\rm bare}/u_0^4$ (tadpole-improved using the plaquette, $u_0 = \langle U_{\mu\nu}\rangle^{1/4}$) parametrizes the logarithmic dependence on the lattice spacing; see Fig. 2. For lattice spacings coarser than $a \lesssim 0.04\,$fm some higher order terms in $(\alpha_s^{\rm lat})^j$ or $(am_{h0})^{2n}$ have to be included in a fit, i.e. see Ref. [12] for a detailed discussion of the continuum extrapolation with up to eleven lattice spacings in the range $0.025\,{\rm fm} \lesssim a \lesssim 0.109\,$fm. Such sophisticated analyses indicate the upward curvature for R_4, and the downward curvature for the ratios R_6/R_8, or R_8/R_{10} in the approach to the continuum limit for all heavy valence quark masses; see Fig. 2. For the higher moments R_n/m_{h0} $(n \geq 6)$ no curvature can be resolved, since the error budget is dominated by lattice scale, r_1/a. The continuum extrapolated results of the most recent valence HISQ results [12] on the (2+1)-flavor HISQ ensembles can be found in Tables 5 and 6 of Ref. [12]. Since sea quark effects are insignificant, these results can be considered as corresponding to physical sea quarks.

$\alpha_s(m_h)$ can be obtained by fitting the continuum results of R_4, R_6/R_8, or R_8/R_{10} with Eq. (3.4). Using the thus obtained result $\alpha_s(m_h)$ in Eq. (3.4) for the higher moments $m_h(m_h)$ can be calculated. Finally, combining $\alpha_s(m_h)$ and $m_h(m_h)$ in the perturbative running one finally obtains the QCD

Lambda parameter $\Lambda_{\overline{\rm MS}}(N_f=3)$, which can be converted to $\alpha_s(M_Z)$, see Ref. [12] for a detailed discussion of these individual results, the error budget, and the details of the perturbative running and matching. In summary, the spread between the results for $\Lambda_{\overline{\rm MS}}(N_f=3)$ at $m_h=m_c,\ 1.5m_c,\ 2m_c$ and $3m_c$ is larger than the individual error estimates, which might hint at difficulties with the continuum extrapolation for the larger quark masses. Taking the spread as a conservative estimate of the error of the unweighted average we obtain after running to M_Z

$$\alpha_s(M_Z) = 0.1159(12), \tag{3.6}$$

while restriction to $m_h \leq 1.5m_c$ results in $\alpha_s(M_Z) = 0.1166(7)$, which is consistent with Eq. (3.6). On the contrary, the determination of the heavy quark masses is without complications. Combining the error of r_1 with the $m_h(m_h)$ results, we obtain the $\overline{\rm MS}$ charm and bottom quark masses as

$$m_c(m_c,N_f=4) = 1.265(10)\,\text{GeV}, \qquad m_b(m_b,N_f=5) = 4.188(37)\,\text{GeV}. \tag{3.7}$$

4. Conclusions

On the one hand, the results for the heavy quark masses obtained from the moments of quarkonium correlators are in excellent agreement with other results determined from lattice QCD [14]. On the other hand, the results for the strong coupling constant from the QCD static energy and from the moments of quarkonium correlators are lower but marginally consistent with most other results determined from lattice QCD [14], but agree with each other quite well. Part of the spread may be due to the difficulty of the continuum extrapolation with the logarithmic lattice spacing dependence. Obvious routes to alleviating these issues might be a calculation of reduced moments or the static energy before the nonperturbative correction at the one-loop level instead of the tree-level or a simultaneous continuum extrapolation of the moments for different heavy quark masses.

References

[1] A. Bazavov *et al.* [HotQCD Collaboration], Phys. Rev. D **90**, 094503 (2014)

[2] A. Bazavov, P. Petreczky and J. H. Weber, Phys. Rev. D **97**, no. 1, 014510 (2018).

[3] M. Berwein, N. Brambilla, P. Petreczky and A. Vairo, Phys. Rev. D **96**, no. 1, 014025 (2017).

[4] A. Bazavov *et al.* [TUMQCD Collaboration], Phys. Rev. D **98**, no. 5, 054511 (2018).

[5] A. Bazavov *et al.* [TUMQCD Collaboration], Phys. Rev. D **100**, no. 11, 114511 (2019).

[6] A. Bazavov *et al.*, Phys. Rev. D **90**, no. 7, 074038 (2014).

[7] I. Allison *et al.* [HPQCD Collaboration], Phys. Rev. D **78**, 054513 (2008).

[8] D. J. Broadhurst, P. A. Baikov, V. A. Ilyin, J. Fleischer, O. V. Tarasov and V. A. Smirnov, Phys. Lett. B **329**, 103 (1994).

[9] B. V. Geshkenbein, B. L. Ioffe and K. N. Zyablyuk, Phys. Rev. D **64**, 093009 (2001).

[10] B. Dehnadi, A. H. Hoang and V. Mateu, JHEP **1508**, 155 (2015).

[11] D. Boito and V. Mateu, arXiv:1912.06237 [hep-ph].

[12] P. Petreczky and J. H. Weber, Phys. Rev. D **100**, no. 3, 034519 (2019).

[13] B. Chakraborty *et al.*, Phys. Rev. D **91**, no. 5, 054508 (2015).

[14] J. Komijani, P. Petreczky and J. H. Weber, *in preparation*.

PoS(LATTICE2019)101